



1                                   **On surface fluxes at night – the virtual chamber approach.**

2   Bruce B. Hicks<sup>1</sup>, Nebila Lichiheb<sup>2</sup>, Deb L. O’Dell<sup>3</sup>, Joel Oetting<sup>3</sup>, Neal S. Eash<sup>3</sup>, Mark Heuer<sup>2,4</sup>,  
3   Latoya Myles<sup>2</sup>

4   <sup>1</sup>*MetCorps, PO Box 1510, Norris, TN 37828, USA*

5   <sup>2</sup>*National Oceanic and Atmospheric Administration, Atmospheric Turbulence and Diffusion Division, Oak  
6   Ridge, TN 37831-2456, USA*

7   <sup>3</sup>*Institute of Agriculture, University of Tennessee, 2506 E.J. Chapman Drive, Knoxville, TN 37996, USA*

8   <sup>4</sup>*Oak Ridge Associated Universities, Oak Ridge, TN 37830, USA*

9  
10   **Abstract**

11   Quantification of the emission rates of various gases from soils at night remains a challenge,  
12   confronting climate science (in the case of CO<sub>2</sub> and CH<sub>4</sub>) and agriculture science (for NH<sub>3</sub> and  
13   N<sub>2</sub>O, among others). In sufficiently stable conditions at night, concentrations of such emitted  
14   gases build up at the surface, with intermittent interruptions commonly attributed to the  
15   passage of packets of turbulence. The utility of conventional micrometeorological experimental  
16   methods in such circumstances is questionable, and chamber methods have been developed to  
17   meet the challenge. Here, a statistical approach is proposed, in which micrometeorological  
18   field data are used to replicate the likely characteristics of a chamber experiment, yielding  
19   estimates of surface fluxes at the surface itself rather than at some height above it. The  
20   methodology proposed is developmental at this time, with details intended to correspond to  
21   the use of both closed and vented chambers. Its application to three recent field studies is  
22   explored: (1) a study of nocturnal CO<sub>2</sub> emission from two test areas (one previously tilled and  
23   the other not) in Ohio in 2015; (2) a similar experiment conducted in Zimbabwe in 2013 (one  
24   area previously tilled and a second left fallow), and (3) an investigation of NH<sub>3</sub> effluxes from a  
25   crop previously treated with urea ammonium nitrate (UAN), in Illinois in 2014. There are few  
26   measurements with which to compare the results presented here, however the values obtained  
27   are within the range of available field data.

28

29   **Keywords:** Soil efflux, CO<sub>2</sub>, CH<sub>4</sub>, NH<sub>3</sub>, nocturnal intermittency, Zimbabwe

30



31 **1. Introduction**

32 Quantification of the emission rates of trace gases from soils in fields, wetlands and forests  
33 presents a problem that standard micrometeorological methods fail to solve (Skiba et al., 2009;  
34 Wilson et al., 2012). While eddy correlation techniques, in their various forms, have gained  
35 popularity, their requirement for sufficient fetch remains an obstacle that is difficult to  
36 overcome, especially at night (Aubinet, 2008). Bowen ratio methods are less susceptible to  
37 fetch limitations, because relevant measurements can be made at a lower height than for eddy  
38 correlation or flux/gradient calculations (Meyers et al., 1996).

39 Measurement of fluxes at night is especially demanding (Schneider et al., 2009; Darenova et al.,  
40 2014). While sensitivity to fetch limitations is reduced, the Bowen ratio methods remain fallible  
41 at night, when the inherent assumption that gradients and fluxes are closely associated is  
42 vulnerable. To address the matter of emissions from soils at night, field programs often rely on  
43 measurement methods of an entirely different kind – the use of chambers that confine  
44 emissions from the ground within closely-monitored volumes and thus eliminating the  
45 problems associated with fetch. In the case of carbon dioxide (CO<sub>2</sub>), for example, the rate of  
46 increase in CO<sub>2</sub> concentrations within such a confined volume is an indication of the flux from  
47 the surface. However, it is recognized that the presence of any such chamber imposes an  
48 obstacle to the natural flow regime, with consequences that are hard to quantify. On the  
49 whole, there is no method that appears to satisfy the objections of all critics.

50 Comparisons among results obtained using chambers of different configurations have been  
51 revealing. Comparison of results from closed ('static', q.v. Edwards, 1982) chambers and  
52 alternative 'dynamic' approaches (Norman et al., 1992) has received particular attention. Field



53 studies summarized by Nay et al. (1994) have indicated considerable differences, sufficient that  
54 laboratory tests were conducted of their performance involving the measurement of CO<sub>2</sub> efflux  
55 rates of known magnitude from test surfaces. The laboratory evaluations confirmed the level of  
56 uncertainty derived from the many field comparisons, with differences sometimes exceeding a  
57 factor of two. A more extensive examination was reported by Pumpanen et al. (2004), whose  
58 independent research allowed them to conclude that “Any use of the static-chamber method  
59 ought to be particularly scrutinized.” Wang et al. (2004) compared results from closed and  
60 vented chambers, with results indicating differences in derived soil efflux rates (of ammonia  
61 (NH<sub>3</sub>) in their tests) ranging up to a factor of five.

62 Here, a statistical approach is proposed, replicating the constraints associated with chamber  
63 methods in a way that leads to estimates of average fluxes rather than specific short-term  
64 situations. The present intent is to demonstrate the utility of the methodology, without  
65 proposing that it should replace other experimental methods but indicating the benefits of a  
66 statistical way of looking at the results of field studies.

67 The concept of a ‘virtual chamber’ analysis to derive flux information from nighttime  
68 concentration data (of trace gases like CO<sub>2</sub>, methane (CH<sub>4</sub>), nitrogen oxide (NO<sub>x</sub>), and NH<sub>3</sub>)  
69 arose in examination of data obtained in Zimbabwe, which illustrated the ramp structure at  
70 night considered due to dilution of CO<sub>2</sub> accumulation in the stratified layers of air near the  
71 surface by nocturnal intermittent turbulence (Hicks et al., 2015). The Zimbabwe dataset is of  
72 special interest, because it relates to a field site on the arid Zimbabwe plateau near Harare, at  
73 an altitude of more than 1400 m asl. The Zimbabwe dataset will be revisited below, as one of  
74 the three examples of the analysis methodology now proposed.



75 **2. The virtual chamber**

76 Consider the case of trace gas emission from a specific surface. At this point, there is no  
77 consideration of the conventional requirement for time stationarity and spatial uniformity.  
78 These issues will be considered later. In daytime convective (and unstable) situations, the  
79 measurement of the fluxes is typically considered as a standard micrometeorological exercise.  
80 At night, however, the constraints imposed by the necessary assumption that fluxes measured  
81 in the air at some convenient height above a surface of special interest are indeed  
82 representative of that particular surface presents substantial obstacles (Aubinet, 2008). It is the  
83 nocturnal stratified atmosphere in contact with the surface that will be considered here.

84 There are many published examples of nighttime time series of measurements of concentration  
85 of some gas (e.g. CO<sub>2</sub> or CH<sub>4</sub>) in ground-level air that displays a saw-tooth pattern, with slowly  
86 increasing concentrations interrupted by sharp decreases (Wehr et al., 2013). These  
87 intermittent decreases are commonly attributed to bursts of turbulence interrupting an  
88 otherwise quiescent surface boundary layer. There are several possible causes of these  
89 turbulent events, such as the oscillations of a low-level jet or the generation of gravity waves by  
90 some upwind obstacle (Aubinet, 2008; Mahrt et al., 2019). It is possible that the phenomena  
91 are a basic feature of strongly stratified flow (Manneville and Pomeau, 1979; He and Basu,  
92 2015), as a consequence of interactions among different processes (Lorenz, 1963). The related  
93 phenomena are almost invariably external to the classical micrometeorological framework, in  
94 which turbulence is associated with the characteristics of the local surface. The optimal time  
95 resolution is therefore not associated with conventional micrometeorological examinations of  
96 fluxes and gradients, but instead short enough to identify with clarity occasions of



97 intermittency so that these can be excluded from the analysis now proposed -- intended to  
98 focus on the causes of increases in surface concentrations. Field experience indicates that a  
99 time resolution of the trace gas concentration record should best be such that events shorter  
100 than five minutes can be resolved.

101 Suppose a fast-response anemometer is deployed at some convenient height, providing three-  
102 dimensional velocity data (means and variances) every five minutes, or over some alternative  
103 averaging time deemed appropriate. Simultaneously, measurements of concentration (C) of  
104 some atmospheric trace constituent are made, at some point below the sonic installation. After  
105 data accumulation extending over many days, consider the statistical characteristics of  
106 ensembles of data generated after sorting according to time of day. A partial correlation  
107 examination of three variables is of present relevance:

$$108 \quad X_1 = dC/dt \quad (1)$$

$$109 \quad X_2 = u \quad (2)$$

$$110 \quad X_3 = \sigma_w \quad (3)$$

111 where notation is conventional. In practice, the wind speed  $u$  is an output of the sonic  
112 anemometer, as is the standard deviation of the vertical wind component  $\sigma_w$ . The rate of  
113 change of concentration,  $dC/dt$ , is conveniently computed from the initial time sequence of  
114 measurement as:

$$115 \quad dC/dt = (C_{n+1} - C_{n-1}) / (t_{n+1} - t_{n-1}) \quad (4)$$

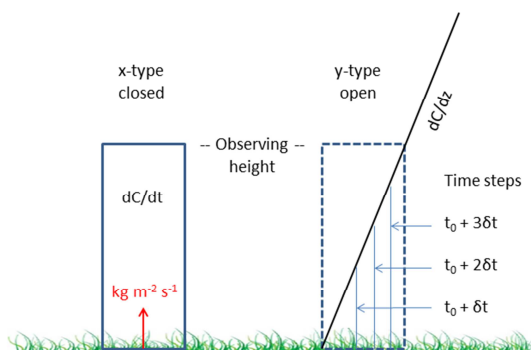


116 A first-order partial correlation analysis (or multiple regressions) yields the best-fitting  
117 coefficients in a relationship of the kind:

$$118 \quad X_1 = a_x + b_{x12} \cdot X_2 + b_{x13} \cdot X_3 \quad (5)$$

119 The intercept  $a_x$  is therefore the value of  $X_1$  (i.e.  $dC/dt$ ) that would be expected in the case for  
120 which  $X_2$  and  $X_3$  were both zero; i.e., for when there is no effect of the wind (no advection) and  
121 no turbulent exchange in the vertical at the level of the anemometer ( $z_a$ ). The situation then  
122 envisioned is that of a conventional closed-chamber experiment, but lacking the consequences  
123 of a physical presence that could influence the natural circumstances.

124 Figure 1 presents a schematic illustration of the construct now considered. Two configurations  
125 are illustrated. Consider, first, the closed-chamber option as discussed above and as illustrated  
126 to the left of the diagram. Clearly, the assumption that a positive value of  $dC/dt$  represents the  
127 accumulation of trace gas in the stable layer of relevance warrants examination. In concept,  
128 the quantity  $C$  would best represent the average within the virtual chamber so defined, of  
129 cross-sectional area of  $1 \text{ m}^2$  and of height  $z_a$ . While this conceptual entity is defined in terms of  
130 specific measurable dimensions, its relevant characteristics are now based on the statistical  
131 extrapolation of other observations.



132

133 *Figure 1. A schematic illustration of the concepts proposed. The x-type chamber*  
134 *simulation is represented to the left, leading to an approximation that the efflux at the*  
135 *surface can be derived from measurements of the rate of change of concentration with*  
136 *time. This is considered an extreme case for the limiting statistical analysis now*  
137 *proposed. An alternative y-type extreme is represented to the right, in which the depth*  
138 *of the layer of relevance is allowed to grow while maintaining the same concentration*  
139 *gradient.*

140

141 The assumption that  $dC/dt$  is the appropriate revealing quantity in the present closed-chamber  
142 context requires further attention. It is considered here to represent an extreme circumstance  
143 controlling the statistics that follow. An alternative extreme might well simulate an open  
144 chamber, in which the depth of the affected layer increases with time, according to the flux  
145 from the surface, but maintaining a constant gradient in the air. In this alternative hypothetical  
146 case, the concentration observed at some height at or below  $z_a$  will increase as the square root  
147 of elapsed time (as is illustrated in Figure 1), rather than linearly as required by the closed-



148 chamber approach. Hence, the conceptual virtual chamber can be considered in two ways,  
149 representing extremes. The first ('x-type') makes use of  $dC/dt$  as a key variable, with  
150 conceptual association with the operation of a closed but stirred chamber. The second ('y-  
151 type') is intended to simulate the characteristics of an open chamber, by substituting  $Y_1 =$   
152  $(dC/dt)^2$  for  $X_1 = dC/dt$  in the discussion above (specifically in Equation (1)). In this second case,  
153 the eventual relationship sought is

$$154 \quad Y_1 = a_y + b_{y12} \cdot X_2 + b_{y13} \cdot X_3 \quad (6)$$

155 which replicates Equation (5). The two separate estimates of the ensemble-mean average  
156 fluxes are then

$$157 \quad F_x = z_a \cdot a_x. \quad (7)$$

$$158 \quad \text{and} \quad F_y = z_a \cdot a_y^{0.5} / 2 \quad (8)$$

159 where the divisor arises from the consideration of a right-triangular conceptual configuration in  
160 the second case (as is evident in Figure 1), rather than the rectangular figure that contains it in  
161 the former.

162 Regardless of the assumption adopted, a measure of the depth of the layer of relevance is a  
163 central requirement. Here, this depth is assumed to be the level at which the loss vertically is  
164 indicated to trend to zero – the height of measurement of  $\sigma_w$  or of some other convenient  
165 indicator of minimal vertical turbulent exchange. Virtual temperature gradients or TKE could be  
166 used equivalently. (Note, however, that the intent to consider the limit as transfer to air above  
167 trends to zero requires that the temperature gradient variable of relevance should be the



168 inverse of the virtual potential temperature gradient, i.e. determining the limit as  $\delta T_v$  tends to  
169 infinity.) The inclusion of wind speed is in recognition of the desire to eliminate advection as a  
170 major causative property, even though if the site in question is sufficiently uniform the wind  
171 speed contribution would be expected to become negligible. If fetch is limited and if the flux of  
172 interest can be associated solely with that fetch, then  $u/X_f$  becomes an attractive variable,  
173 where  $X_f$  is the upwind fetch.

174 In the analysis to follow, two distinct methodologies are proposed. The x-analysis as outlined  
175 above assumes that changes in concentration in air near the surface can be considered as being  
176 proportional to changes in the surface fluxes. The corresponding y-analysis replaces  $X_1$  by  $Y_1 =$   
177  $X_1^2$  (q.v. Figure 1) and assumes that changes in concentration measured at some specific height  
178 are determined by changes in the depth of the surface stable layer, such that the concentration  
179 gradient remains the same.

180 In practice, the requisite analysis employs standard statistical methods, adapted from textbook  
181 examples (in which matrix algebra is commonly employed) for the present simple case by  
182 evaluating the correlation coefficients of relevance ( $R_{12}$  is the correlation coefficient between  
183 variables  $X_1$  and  $X_2$ ) and the resulting partial correlations ( $R_{12.3}$  is the partial correlation between  
184 variable  $X_1$  and  $X_2$  when the influence of variable  $X_3$  is accounted for). Of considerable relevance  
185 in analyses like that presented here are the consequent quantities

186 
$$R_{1.23}^2 = R_{12.3}^2(1 - R_{13}^2) + R_{13}^2 \quad (9)$$

187 
$$R_{1.32}^2 = R_{31.2}^2(1 - R_{12}^2) + R_{12}^2 \quad (10)$$



188 which quantify the proportion of the variance in variable  $X_1$  that can be explained by the  
189 combination of variables  $X_2$  and  $X_3$ . Finding the equality evident in the two ways of deriving  
190 this quantity is a confidence-building exercise of some considerable satisfaction.

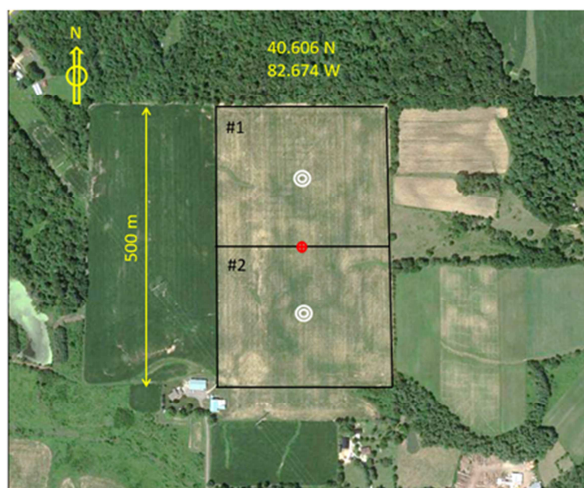
191 Standard statistical relationships lead immediately to the quantification of the variables  $\alpha_x$  and  
192  $\alpha_y$  in Eqs. (5) and (6). Estimates of the effluxes then derive immediately, assuming that the  
193 height of measurement determines the average height used to define the conceptual chamber  
194 of relevance. This is a statistical matter that invites further examination.

195 In neither the closed-chamber or the open-chamber approximation can the results be  
196 considered actual measurements of the surface efflux rates. They are no more than statistical  
197 estimates of these fluxes, based on numerically quantified heurism. Conventional experimental  
198 campaigns typically provide bodies of suitable data. In the following, three examples of recent  
199 application of the virtual chamber approach will be described. The first of these relates to a  
200 study of the consequences of tilling on the emissions of  $\text{CO}_2$  from an agricultural surface in  
201 central Ohio (O'Dell et al., 2018). The measurement program was based on standard Bowen  
202 Ratio Energy Balance protocols. The second repeats the analysis, using similar data derived  
203 from an earlier study conducted in Zimbabwe (Hicks et al, 2015, O'Dell et al, 2015). The third is  
204 based on a study of ammonia emissions from an area previously treated with urea-ammonium  
205 nitrate (UAN) as a nitrogenous fertilizer in central Illinois (Nelson et al., 2017, 2019). These  
206 examples were selected for present attention because the dimensions of the subject areas are  
207 sufficiently small that conventional nighttime micrometeorological methods are not likely to be  
208 productive.



209 **3. The Ohio study of tilling**

210 Figure 2 (a) shows the layout of the field site of the Ohio study (O'Dell et al., 2015).  
211 Measurements were made of the concentration of CO<sub>2</sub> in the air, the air temperature and  
212 vapor pressure at two levels close to the surface, wind speed, and the surface temperature as  
213 reported by downward looking infrared thermometers. The central question related to whether  
214 previous tilling of the surface exacerbated CO<sub>2</sub> emissions from the soil at night. The  
215 experimental program involved the collection of data from two adjacent areas (as seen in  
216 Figure 2), each about 200 m x 200m in size. One of these test areas was tilled (#1), and the  
217 other not tilled (#2) before maize (*Zea mays* L.) was planted. The data were collected in  
218 November 2015, during the immediate post-harvest period. Observations used here were  
219 obtained centrally within each of the study areas, with a time resolution of five minutes.  
220 Experimental constraints caused this resolution to be adjusted, so that the data used here  
221 represent ten-minute intervals.



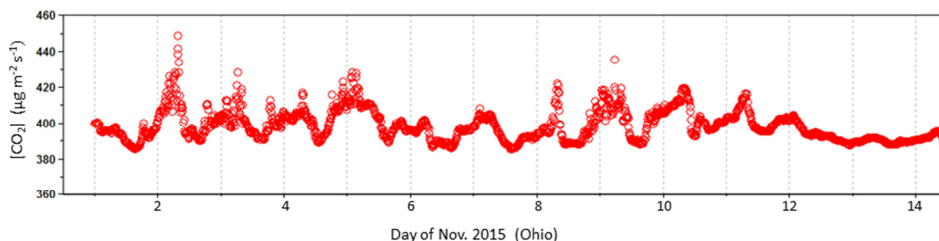
222



223 *Figure 2. The surface layout of the test areas of the Ohio (2015) field study. Stars indicate*  
224 *the locations of measurement systems. The image is derived from copyright © Google*  
225 *Earth.*

226

227 The selection of data for use in the present study has been based on the requirements of the  
228 concepts involved. First, nighttime data must be considered. Hence, data records with reported  
229 positive net radiation have been excluded. Further, the intent was to interpret the increases in  
230 concentration observed near the surface in stable conditions. To this end, situations in which  
231  $dC/dt < 0$  have been rejected (since such situations are likely the consequence of nocturnal  
232 turbulence intermittency, another controlling mechanism to be considered elsewhere). In the  
233 absence of sonic anemometer data, measurements of the virtual temperature gradient derived  
234 from the conventional Bowen ratio energy balance (BREB) methodology have been used. To  
235 quantify the limit as vertical mixing approaches zero,  $X_2$  has been taken to be  $(\delta\theta_v)^{-1}$ , where  $\delta\theta_v$   
236 is the difference between levels  $z_1$  and  $z_2$  (above the ground) of the measured virtual potential  
237 temperature. In the present case,  $z_1$  is about 0.3 m and  $z_2$  about 1.8 m, so that the effective  
238 height to be used in the estimation of fluxes from the evaluations of  $a_x$  and  $a_y$  is about 1 m.



239



240 *Figure 3. Time trends of CO<sub>2</sub> concentration at a height of about 1 m above a recently*  
241 *harvested maize field in Ohio.*

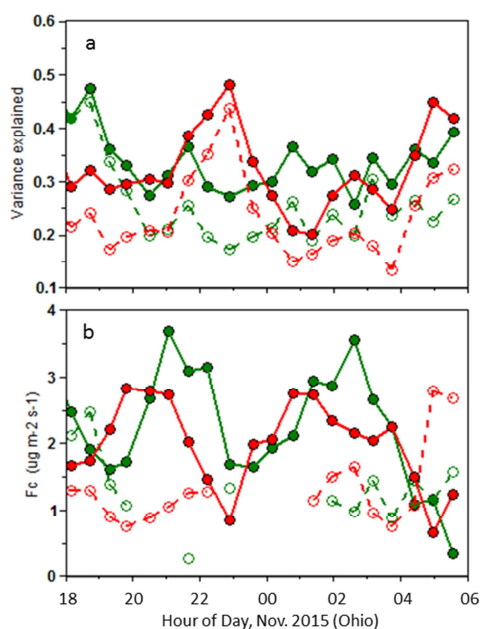
242 Figure 3 presents a sample time record of CO<sub>2</sub> concentrations from the Ohio experiment,  
243 obtained above the untilled field. The characteristic nighttime concentration build-ups are  
244 obvious, as are the consequences of intermittent turbulence. The mid-American farmlands  
245 (within which the present Ohio field site was located) are notorious homes of frequent  
246 nocturnal jets, with consequences that include the generation of irregular bursts of turbulence  
247 (q.v. Blackadar, 1957; Banta, 2008). It is assumed here that it is such irregular bursts of  
248 turbulence that curtail the otherwise steady accumulation of CO<sub>2</sub> in the atmospheric boundary  
249 layer adjacent to the surface. The present intent is not to investigate these bursts of  
250 turbulence, but instead to accept them as features of the nighttime atmospheric environment  
251 and then to examine the trends with time when they are not dominant factors.

252 Figure 4 summarizes results obtained from application of the virtual chamber analysis  
253 methodology outlined above. In Figure 4 (a), plots are shown of the proportion of the variance  
254 in  $X_1$  and likewise in  $Y_1$  that can be accounted for by consideration of variables  $X_2$  and  $X_3$   
255 (following Eqs. (9) and (10)). If this proportion is close to unity, then the data constitute a sound  
256 basis for examination in the way now suggested. However, such high values are not often  
257 encountered in the surface boundary layer atmosphere. For example, the relationship between  
258 wind speed and the surface stress is usually quantified by a correlation coefficient of the order  
259 of 0.4, so that less than 20% of the variance in stress is accounted for by changes in the wind  
260 speed. In this light, the values plotted in Figure 4 (a) are somewhat reassuring, ranging from



261 about 20% to 40%. It is noticeable, however, that the values associated with the open chamber  
262 (y-type) assumption are lower than those of the closed chamber kind (x-type).

263 Figure 4 (b) presents the estimates of surface effluxes derived from the present analysis. There  
264 being no obvious reason to prefer one of the two kinds of analysis rather than the other, it is  
265 presently preferred to accept both and to view them as extremes. It could be argued that  
266 Figure 4 (a) indicates that x-type must be preferred to y-type, but a conclusion of this kind  
267 would require multiple tests and is certainly premature at present. The best estimate of the  
268 average surface emission rate is therefore likely to be the average of all of the values plotted:  
269 For the tilled surface,  $1.70 \pm 0.31 \mu\text{g m}^{-2} \text{s}^{-1}$ , and for the untilled,  $1.33 \pm 0.08 \mu\text{g m}^{-2} \text{s}^{-1}$ . The  
270 most likely averages of CO<sub>2</sub> nocturnal emissions from Ohio agricultural soils are therefore  
271 indicated to be about  $2 \mu\text{g m}^{-2} \text{s}^{-1}$  for the conditions of the current test, regardless of whether  
272 the surface was previously tilled.



273

274 *Figure 4. (a) The variation with time of the proportion of variance in  $dC/dt$  (= X1; ‘closed*  
275 *chamber’) and  $(dC/dt)^2$  (= Y1; ‘open chamber’) that can be accounted for by statistical*  
276 *consideration of the virtual temperature gradient (employed as its inverse,  $1/\delta T_v$ ) and*  
277 *wind speed ( $u$ ), for the two areas of present interest – one tilled before seeding (green)*  
278 *and the other not tilled (red). (b) the estimates of surface effluxes derived from the same*  
279 *analysis. As elsewhere, solid points indicate results obtained using the closed-chamber*  
280 *approximation described here, open points represent vented chamber approximations.*

281

282 **4. The Zimbabwe plateau data**



283 A field examination of the comparative benefits of various agricultural practices was conducted  
284 in Zimbabwe, starting in 2013 (O'Dell et al., 2015, Hicks et al., 2015). Identical BREB  
285 instrumentation was set up centrally in four neighboring experimental areas, of which two will  
286 be considered here (identified as #1 and #2 in the site depiction in Figure 5).



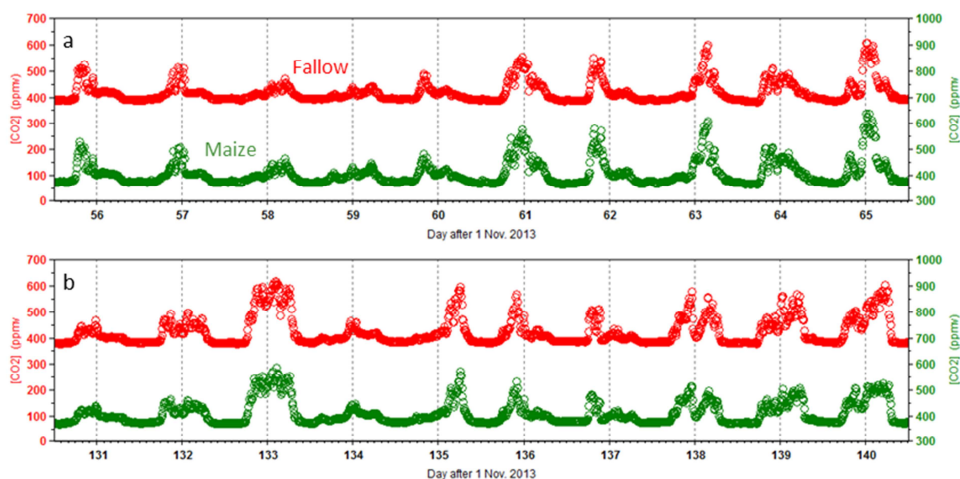
287

288 *Figure 5. The field site of the Zimbabwe study, showing the two test areas, 1 and 2,*  
289 *considered in the present analysis. At the time of the analysis to follow, area 1 was*  
290 *fallow and area 2 was plated with maize. The inset locates to field site within the*  
291 *African continent (31.021E, 17.722S). Both images derive from copyright © Google*  
292 *Earth.*

293



294 An earlier analysis focused on the nocturnal data obtained, with a time resolution of five  
295 minutes so that occurrences of intermittent turbulence were readily apparent (Hicks et al.,  
296 2015). In the lack of major upwind surface irregularities, these occurrences were attributed to  
297 the gravity wave phenomenon considered in detail by Blackadar (1957) but Mahrt et al. (2019)  
298 show that there are several alternative causative mechanisms. The key point of the Zimbabwe  
299 finding was that the site in question was at an altitude of more than 1400 m asl, and the  
300 occurrence of the turbulence intermittency phenomenon at this altitude is a revealing  
301 indication of the ubiquity of the mechanism. The data collection protocols used in the  
302 Zimbabwe study were the same as were used in the Ohio experiment, discussed above. The  
303 analysis now considered for the Zimbabwe dataset mirrors that discussed above for Ohio.



304

305 *Figure 6. Data from the Zimbabwe field site, illustrating the repeated occurrence of a*  
306 *nighttime saw-tooth pattern for two widely-separated periods (selected at random from*  
307 *the overall six-month data record). Values plotted represent ten-minute average CO<sub>2</sub>*



308 *concentrations. Red represents data for the fallow field (#1 in Figure 1), and green the*  
309 *adjacent field (#2) carrying a growing crop of maize. No data have been omitted.*

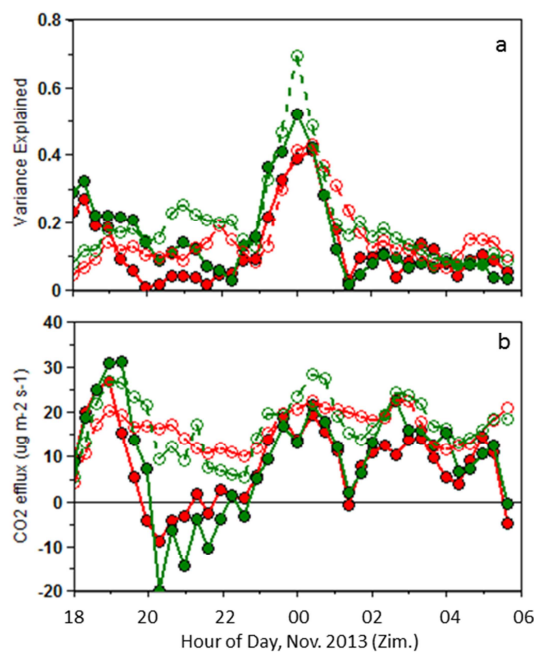
310

311 Figure 6 presents two sequences of CO<sub>2</sub> concentration measurements, obtained above the two  
312 fields of current interest at an average height of about 1 m above the vegetation or soil. The  
313 periods selected for presentation here were selected at random, but are intended to show the  
314 similarity in the overall behavior of the growing maize and the fallow field. Note, however, that  
315 the fallow field carried a coverage of flourishing native weeds, so that any difference could well  
316 have been obscured.

317 Figure 7 replicates Figure 4 using the Zimbabwe data. In Figure 7 (a) it is seen that the  
318 proportion of variance explained is generally low, except for a peak centered on midnight. The  
319 interpretation of this is that the efflux conclusions based on the two-hour window around  
320 midnight are the most robust. In Figure 7 (b) it is clear that the flux estimates are well behaved  
321 for this period, with an average of about 20 μg m<sup>-2</sup> s<sup>-1</sup> of CO<sub>2</sub> emission. As before, there is no  
322 convincing reason to prefer the y-type results over the x-type, even though the negative results  
323 (x-type) indicated in the diagram are disturbing. If all of the results are averaged (as was the  
324 case in consideration of the Ohio dataset), the resulting estimate of the CO<sub>2</sub> efflux for the  
325 Zimbabwe November data is 11.1 ± 1.3 μg m<sup>-2</sup> s<sup>-1</sup> for the area sown with maize, and 10.3 ± 1.5  
326 μg m<sup>-2</sup> s<sup>-1</sup> for the fallow. At the time of these measurements, the maize had not yet fully  
327 emerged and the fallow field was poorly vegetated (with weeds). Concentration and virtual  
328 temperature data refer (as before) to a height of about 1 m above ground level.



329 The test areas used in the Zimbabwe study were smaller than those of Ohio: 80 m on side in  
330 comparison to 200 m. It must be expected that this difference in size will have an effect on the  
331 conclusions derived from the present analyses, although the procedure is designed to be based  
332 on extrapolation of observations to a situation in which the wind speed is zero, at which point  
333 fetch considerations become meaningless.



334

335 *Figure 7. As in Figure 3, with red points relating to a fallow field and green to an*  
336 *adjoining area recently planted with maize (on 8 November, 2013). The dataset*  
337 *development in this case differs, with fewer points making up each ensemble and with*  
338 *consequent increased scatter in the results. The period represented here is the entire*



339 *month of November. Solid points indicate results obtained using the closed-chamber*  
340 *approximation described here, open points represent vented-chamber approximations.*

341

### 342 **5. The Illinois NH<sub>3</sub> study**

343 Nelson et al (2017) reported a study of NH<sub>3</sub> fluxes from an area previously treated with UAN as  
344 a nitrogenous fertilizer. Such treatment is a common practice within the agricultural community  
345 particularly in the Midwestern US. The site is illustrated in Figure 8.



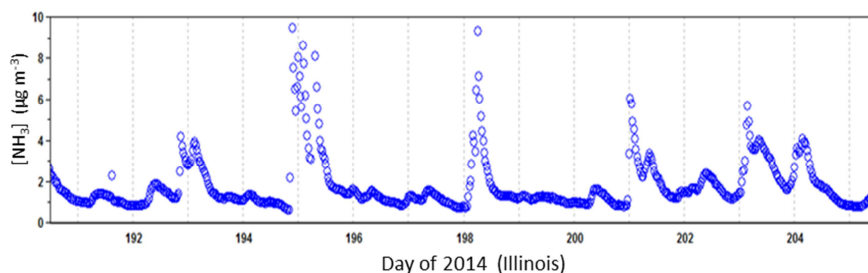
346



347 *Figure 8. As derived from copyright © Google Earth, a map of the 4-ha field site used in*  
348 *the Illinois (2014) study of ammonia fluxes following fertilization using urea ammonium*  
349 *nitrate.*

350

351 Classical investigations of this issue have relied on gross measurements of changes in soil  
352 nitrogen content, typically over periods of weeks. The results of such measurements are highly  
353 influenced by external factors, especially rainfall. The Illinois study of interest here was  
354 intended to explore the micrometeorological use of new fast-response ammonia sensors. In the  
355 process, time series of  $\text{NH}_3$  concentrations near the ground were derived, illustrated in Figure 9,  
356 which constitute a basis for exploration using the virtual chamber methods now proposed. Like  
357 the Ohio experimental area considered above, the Illinois site is within the mid-American  
358 farmlands and is subject to characteristic nocturnal jets and consequent bursts of turbulence  
359 occurring at night (as have been investigated in detail by Banta, 2008, for example). Ammonia  
360 gas measurements made at the Illinois site in 2014 reveal precisely the cyclical pattern  
361 expected to result from such turbulence intermittency, as is seen in Figure 9. The opportunity  
362 exists, therefore, to make use of the analytical methods suggested here in order to derive  
363 information regarding the rate of emanation of ammonia gas from the previously fertilized  
364 area, so as to derive flux data not influenced by rainfall itself but such that the influence of  
365 factors like soil moisture content and temperature could perhaps be assessed.



366

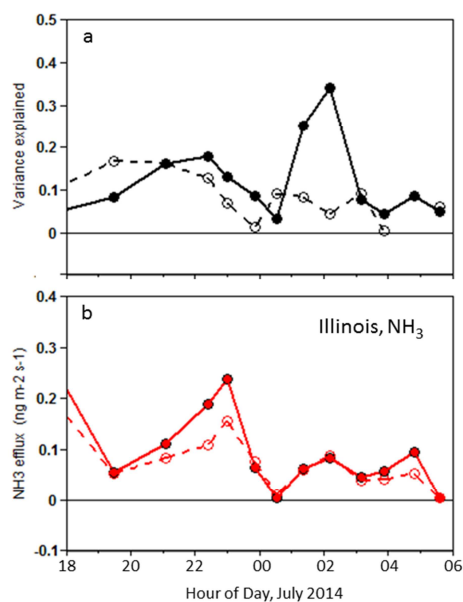
367 *Figure 9. A time sequence of NH<sub>3</sub> concentration measurements obtained in the 2014*  
368 *Illinois field study.*

369

370 Using a two-week period of data (of which Figure 9 is representative), results obtained using  
371 the virtual chamber approach are as indicated in Figure 10. A key distinction between the  
372 present ammonia case and the CO<sub>2</sub> examples considered above is that the NH<sub>3</sub> concentrations  
373 are available as 30-min averages, instead of the 10-min averages used for the Ohio and  
374 Zimbabwe datasets. The consequences of this are apparent in Figure 10 (a), where the total  
375 proportion of variance explained in the rate of change of NH<sub>3</sub> concentration with time is lower  
376 than that derived for the CO<sub>2</sub> cases. It is clear that the methods considered here require finer  
377 time resolution than is common for conventional micrometeorological studies, since the overall  
378 intent is now to detect and omit situations in which intermittent bursts of turbulence affect the  
379 buildup of concentrations in the layer of stratified air in immediate contact with the surface.  
380 Reliance on data that fail to permit fine distinction between periods of turbulence bursting and  
381 the quiescent periods between successive intermittent bursts occurrences certainly obscures



382 the statistical correlations on which the present techniques are based, and will result in an  
383 underestimation of the efflux in question.



384

385 *Figure 10. Results derived from measurements of NH<sub>3</sub> above a field previously fertilized*  
386 *with treatment of UAN, in Illinois in 2014. As in the similar presentations above, (a)*  
387 *represents the total proportion of variance explained in dC/dt by the combined*  
388 *influences of wind speed and turbulent mixing, from interpretation of which (b) indicates*  
389 *how derived NH<sub>3</sub> effluxes vary through the night. As before, solid points indicate results*  
390 *obtained using the closed-chamber approximation described here, open points represent*  
391 *vented chamber approximations.*

392

393 **6. Discussion**



394 The present intent has been to make use of several different datasets to illustrate the potential  
395 utility of the virtual chamber analytical methodology and not to focus on results from any  
396 specific location in detail. Nevertheless, it is clear from the analyses above that the CO<sub>2</sub> efflux  
397 from the Zimbabwe site exceeded that from the Ohio location by about an order of magnitude.  
398 The reason is not clear, but several obvious considerations are worthy of attention. For  
399 example, differences in soil temperatures could explain the difference: about 7.5 C for the Ohio  
400 dataset and 24.0 C for the Zimbabwe. Differences in soil moisture are to be expected, and  
401 would likely contribute to the difference. The Ohio surface was covered with the detritus of  
402 recent harvesting, whereas the Zimbabwe surface had been recently planted. All in all, the  
403 situation is complicated and requires more attention than is presently appropriate.

404 Irrespective of the negative consequences imposed by the half-hour sampling associated with  
405 the Illinois dataset, Figure 10 (b) provides a convincing indication that the rate of NH<sub>3</sub> emission  
406 from the ground was about 0.1 ng m<sup>-2</sup> s<sup>-1</sup>. Wang et al. (2004) report results that indicate that  
407 the rate of volatilization of ammonia from an area bearing a maize crop depended almost  
408 linearly on the amount of urea previously broadcast. The maximum NH<sub>3</sub> emission rate was  
409 about two days following application of the fertilizer, but at an average rate of from 0.1 to 0.8  
410 kg ha<sup>-1</sup> d<sup>-1</sup>, corresponding to about 0.1 to 0.8 μg m<sup>-2</sup> s<sup>-1</sup>. The efflux estimate derived from the  
411 present analysis is three orders of magnitude lower. In all comparisons of this kind, it should be  
412 remembered that the classical chamber study results are typically presented as whole-day  
413 averages, whereas the virtual chamber results bow being considered represent only those  
414 times of the day when the air in contact with the surface is stratified – usually, at night. Once  
415 again, the difference invites investigation.



416

## 417 **7. Conclusions**

418 The methodology presented here diverges substantially from familiar micrometeorological  
419 strategies. First, it is focused on the ground itself (or the vegetation above it), and does not rely  
420 on the assumption that measurements made above the ground are indicative of the local  
421 surface. Second, the reliance on statistical methods to drive the analysis towards situations in  
422 which the prevailing stability is high but the wind speed is zero reduces (if not eliminates) the  
423 conventional requirement regarding large fetches. Third, the method requires measurements  
424 with a sufficient time resolution (less than 5 min) such that the effects of intermittent bursts of  
425 turbulence can be identified and eliminated. This is in direct contrast to standard  
426 micrometeorological practice, which requires a sampling duration long enough that a  
427 statistically significant sampling of these same bursts of turbulence can be obtained.

428 However, the methods now presented do not result in a defensibly deterministic quantification  
429 of the relevant surface fluxes. It is assumed that the two alternative methods presented and  
430 discussed above represent extremes, so that the exchange rates of actual relevance lie between  
431 the corresponding bounds. A similar line of thinking was proposed by Wang et al. (2004), who  
432 report on results obtained from field studies over the North China Plain using both closed and  
433 vented chambers. These two experimental methods yielded flux estimates that differed by as  
434 much as an order of magnitude. Hence, the differences found in the studies now considered  
435 appear reasonable, although clearly requiring additional research.

436



437 **Acknowledgements**

438 The authors gratefully acknowledge funding from the National Science Foundation (Award  
439 Numbers AGS12-36814 and AGS 12-33458) for the Illinois study. The scientific results and  
440 conclusions, as well as any views or opinions expressed herein, are those of the authors and do  
441 not necessarily reflect the views of NOAA, the Department of Commerce, or NSF.

442



#### 443 References

- 444 Aubinet, M.: Eddy Covariance CO<sub>2</sub> Flux Measurements in Nocturnal Conditions: An Analysis of  
445 the Problem, *Ecol. Appl.*, 18, 1368-1378, 2008.
- 446 Banta, R. M.: Stable-boundary-layer regimes from the perspective of the low-level jet. *Acta*  
447 *Geophys.*, 56, 58-87, 2008.
- 448 Blackadar, A. K.: Boundary layer wind maxima and their significance for the growth of nocturnal  
449 inversions, *Bull. Amer. Meteorol. Soc.*, 38, 283-290, 1957.
- 450 Costa, F. D., Acevedo, O. C., Mombach, J. C. M. and Degrazia, G. A.: A simplified model for  
451 intermittent turbulence in the nocturnal boundary layer, *J. Atmos. Sci.*, 68, 1714-1729,  
452 2011.
- 453 Darenova, E., Pavelka, M., and Acosta, M.: Diurnal deviations in the relationship between CO<sub>2</sub>  
454 efflux and temperature: A case study, *CATENA*, 123, 263-269, 2014.
- 455 Edwards, N. T.: The use of soda-lime for measuring respiration rates in terrestrial systems,  
456 *Pedobiologia*, 23, 321-330, 1982.
- 457 He, P. and Basu, S.: Direct numerical simulation of intermittent turbulence under stably  
458 stratified conditions. *Nonlin. Processes Geophys.*, 22, 447-441, 2015.
- 459 Hicks, B. B., O'Dell, D. L., Eash, N. S., and Sauer, T.: Nocturnal intermittency in surface CO<sub>2</sub>  
460 concentrations in Sub-Saharan Africa, *Agric. and Forest Meteorol.*, 25, 129-134, 2015.
- 461 Lorenz, E. N.: Deterministic nonperiodic flow, *J. Atmos. Sci.*, 20, 130-141, 1963.
- 462 Lorenz, E. N.: The predictability of a flow which possesses many scales of motion, *Tellus*, 21,  
463 289-307, 1969.
- 464 Mahrt, L., Pfister, L. and Thomas, C. K.: Small-scale variability in the nocturnal boundary layer,  
465 *Boundary-Layer Meteorol.*, 172. <https://doi.org/s10546-019-00476-x>.
- 466 Manneville, P. and Pomeau, Y.: Intermittency and the Lorenz model, *Phys. Letters*, 75A, 1-2,  
467 1979.
- 468 Meyers, T. P., Hall, M. E., Lindberg, S. E. and Kim, K. I.: Use of the modified Bowen-ratio  
469 technique to measure fluxes of trace gases, *Atmos. Environ.*, 30, 3321-3329, 1996.
- 470 Nay, S. M., Mattson, K. G. and Bormann, B. T.: Biases of chamber methods for measuring soil  
471 CO<sub>2</sub> efflux demonstrated with a laboratory apparatus, *Ecology*, 75, 2460-2463, 1994.
- 472 Nelson, A. J., Koloutsou-Vakakis, S., Rood, M. J., Myles, L., Lehmann, C., Bernacchi, C.,  
473 Balasubramanian, S., Joo, E., Heuer, M., Vieira-Filho, M., Lin, J.: Season-long ammonia  
474 flux measurements above fertilized corn in central Illinois, USA, using relaxed eddy  
475 accumulation, *Agric. and Forest Meteorol.*, 239, 202-212, 2017.
- 476 Nelson, A. J., Lichiheb, N., Koloutsou-Vakakis, S., Rood, M. J., Heuer, M., Myles, L., Joo, E.,  
477 Miller, J., Bernacchi, C.: Ammonia flux measurements above a corn canopy using relaxed  
478 eddy accumulation and a flux gradient system, *Agric. and Forest Meteorol.*, 264, 104-  
479 113, 2019.



- 480 Norman, J. M., Garcia, R. and Verma, S. B.: Soil surface CO<sub>2</sub> fluxes and the carbon budget of  
481 grassland, *J. Geophys. Res.*, 97, 845-18 853, 1992.
- 482 O'Dell, D. L., Sauer, T. J., Hicks, B. B., Thierfelder, C., Lambert, D. M., Logan, J. and Eash, N. S.: A  
483 short-term assessment of carbon dioxide fluxes under contrasting agricultural and soil  
484 management practices in Zimbabwe, *J. Agric. Sci.*, 7, 32-48, 2015.
- 485 O'Dell, D. L., Eash, N. S., Hicks, B. B., Oetting, J. N., Sauer, T. J., Lambert, D. M., Logan, J., Wright,  
486 W. C. and Zahn, J. A.: Reducing CO<sub>2</sub> flux by decreasing tillage in Ohio: overcoming  
487 conjecture with data, *J. Agric. Sci.*, 7, 1-15, 2018.
- 488 Pomeau, Y. and Manneville, P.: Intermittent transition to turbulence in dissipative dynamical  
489 systems, *Commun. Math. Phys.*, 74, 189-197, 1980.
- 490 Pumpanen, J., Kolari, P., Ilvesniemi, H., Minkkinen, K., Vesala, T., Niinistö, S., Lohila, A., Larmola,  
491 T., Morero, M., Pihlatie, M., Janssens, I., Yuste, J. C., Grünzweig, J. M., Reth, S., Subke, J.-  
492 A., Savage, K., Kutsch, W., Ostreng, G., Ziegler, W., Anthoni, P., Lindrotyh, A. and Hari, P.:  
493 Comparison of different chamber techniques for measuring soil CO<sub>2</sub> efflux, *Agric. Forest  
494 Meteorol.*, 123, 159-176, 2004.
- 495 Schneider, J., Kutzbach, L., Schulz, S. and Wilmking, M.: Overestimation of CO<sub>2</sub> respiration fluxes  
496 by the closed chamber method in low-turbulence nighttime conditions, *J. Geophys. Res.:*  
497 *Biogeosci.*, 114, G03005, 2009.
- 498 Skiba, U., Drewer, J., Tang, Y. S., van Dijk, N., Helfter, C., Nemitz, E., Famulari, D., Cape, J. N.,  
499 Jones, S. K., Twigg, M., Pihlatie, M., Vesala, T., Larsen, K. S., Carter, M. S., Ambus, P.,  
500 Ibrom, A., Beier, C., Hensen, A., Frumau, A., Erisman, J. W., Brüggemann, N., Gasche, R.,  
501 Butterbach-Bahl, K., Neftel, A., Spirig, C., Horvath, L., Freibauer, A., Cellier, P., Laville, P.,  
502 Loubet, B., Magliulo, E., Bertolini, T., Seufert, G., Andersson, M., Manca, G., Laurila, T.,  
503 Aurela, M., Lohila, A., Zechmeister-Boltenstern, S., Kitzler, B., Schaufler, G., Siemens, J.,  
504 Kindler, R., Flechard, C. and Sutton, M. A.: Biosphere–atmosphere exchange of reactive  
505 nitrogen and greenhouse gases at the NitroEurope core flux measurement sites:  
506 Measurement strategy and first data sets, *Agric., Ecosyst. & Environ.*, 133, 139-149,  
507 2009.
- 508 Wang, Z.-H., Liu, X.-J., Ju, X.-T., Zhang, F.-S. and Malhi, S. S.: Ammonia volatilization loss from  
509 surface-broadcast urea: Comparison of vented- and closed-chamber methods and loss in  
510 winter wheat-summer maize rotation in North China Plain, *Comm. Soil Sci. and Plant  
511 Anal.*, 35, 2917-2939, 2004.
- 512 Wehr, R., Munger, J. W., Nelson, D. D., McManus, J. B., Zahniser, M. S., Wofsy, S. C. and Saleska,  
513 S. R.: Long-term eddy covariance measurements of the isotopic composition of the  
514 ecosystem–atmosphere exchange of CO<sub>2</sub> in a temperate forest, *Agric. Forest Meteorol.*,  
515 181, 69-84, 2013.



516 Wilson, T. B., Meyers, T. P., Kochendorfer, J., Anderson, M. C. and Heuer, M.: The effect of soil  
517 surface litter residue on energy and carbon fluxes in a deciduous forest, *Agric. Forest*  
518 *Meteorol.*, 161, 134-147,2012.  
519